Structural Transformations in Dinuclear Zinc Complexes Involving Zn-Zn Bonds

Yi-Chou Tsai,[a],*, Duan-Yen Lu[a], Yang-Miin Lin,[a] Jenn-Kang Hwang,[b] and Jen-Shiang K. Yu[b]

[a]Department of Chemistry, National Tsing Hua University, Hsinchu 300, Taiwan, Republic of China,
[b]Department of Biological Science and Technology, National Chiao Tung University, Hsinchu 300, Taiwan, Republic of China
E-mail: yictsai@mx.nthu.edu.tw

Experimental

General Information. Unless stated otherwise, all operations were performed
using standard Schlenk techniques or in a Vacuum Atmospheres dry box under an
atmosphere of nitrogen. Diethyl ether (Et_2O) and tetrahydrofuran (THF) were distilled
under nitrogen from purple sodium benzophenone ketyl. Hexane was distilled under
nitrogen from CaH_2. Distilled solvents were transferred under vacuum into
vacuum-tight glass vessels before being transferred into a drybox. C_6D_6 was
purchased from Aldrich and was degassed and dried over 4 Å sieves. The 4 Å
sieves and Celite were dried in vacuo overnight at a temperature just above 200 °C.
All other compounds were used as received. ^1H and ^{13}C NMR spectra were recorded
on Bruker Avance 400 MHz, Varian Unity INOVA 500 MHz or Bruker DMX 600
MHz spectrometers at room temperature. ^{13}C NMR spectra are proton decoupled.
Chemical shifts are reported with respect to internal solvent: 7.16 ppm (^1H) and
128.00(t) (^{13}C) ppm (C_6D_6). CHN analyses were performed by Precious Instrument
Center at National Chiao Tung University (Hsinchu, Taiwan) with a Heraeus
CHN-O-Papid elemental analyzer.

Synthesis of Zn$_2$(μ-η^2-Me$_2$Si(NDipp)$_2$)$_2$ (5). In a 100 mL of round bottom flask was prepared a suspension of ZnBr$_2$ (2.30 g, 10.20 mmol) in 50 mL of diethyl ether and kept at –35 °C for 30 min. To the suspension was slowly added solid Li$_2$[Me$_2$Si(NDipp)$_2$] (4.35 g, 10.30 mmol) at –35 °C. As the reaction mixture was allowed to warm to room temperature, dissolution of ZnBr$_2$ was observed in 1 hr. Stirring was continued at room temperature overnight, at which point, it was filtered through Celite and all volatiles were removed to dryness under vacuum. Recrystallization from toluene/hexane at –35 °C furnished **5** as colorless crystals. Yield: (2 crops 92%). ^{1}H NMR (600 MHz, C$_6$D$_6$): δ 7.02 (br, 12H, Dipp meta and para), 4.07 (br, 8H, C*H*Me$_2$), 1.30 (br, 24H, CH*Me$_2$*), 1.01 (br, 24H, CH*Me$_2$*), 0.05 (s, 12H, Si*Me$_2$*). ^{13}C NMR (151 MHz, C$_6$D$_6$): δ 146.2 (C, Dipp *ipso*), 141.0 (C, Dipp *ortho*), 124.9 (CH, Dipp *para*), 123.9 (CH, Dipp *meta*), 27.6 (CH, *C*HMe2), 25.8 (CH$_3$, CH*Me$_2$*), 22.7 (CH$_3$, CH*Me$_2$*), 1.80 (CH$_3$, Si*Me$_2$*). Anal. Calcd for C$_{52}$H$_{80}$N$_4$Si$_2$Zn$_2$: C, 65.87; H, 8.50; N, 5.91; Found: C, 65.80; H, 8.20; N, 5.83.

Synthesis of K$_2$[Zn(η^2-SiMe$_2$(NDipp)$_2$)]$_2$ (6). To a solution of **5** (8.27 g, 8.72 mmol) in 80 mL of toluene in a 250 mL of round bottom of flask was slowly added solid KC$_8$ (4.70 g, 34.8 mmol) at −35 °C, and the mixture was allowed to warm to room temperature. Vigorous stirring was continuing overnight. The solution was filtered through Celite, and solvent was removed in vacuo from the filtrate, yielding a white solid. Recrystallization from toluene at −35 °C furnished **6** as colorless crystals (7.58 g, 6.97 mmol, 80% yield in two crops). ^{1}H NMR (500 MHz, C$_6$D$_6$): δ 6.81 (d, 8H, *J* = 7.5 Hz, Dipp meta), 6.37 (t, 4H, *J* = 7.5 Hz, Dipp para), 4.26 (septet, 8H, *J* = 7.0 Hz, C*H*Me$_2$), 1.28 (d, 24H, *J* = 7.0 Hz, CH*Me$_2$*), 1.23 (d, 24H, *J* = 7.0 Hz, CH*Me$_2$*), 0.45 (s, 12H, Si*Me$_2$*). ^{13}C NMR (126MHz, C$_6$D$_6$): δ 154.3 (C, Dipp *ipso*), 144.5 (C,

Dipp *ortho*), 123.3 (CH, Dipp *meta*), 116.3 (CH, Dipp *para*), 27.0 (CH, $CHMe_2$), 25.8

(CH_3, $CHMe_2$), 24.9 (CH_3, $CHMe_2$), 6.29 (CH_3, $SiMe_2$). Anal. Calcd for

$C_{56}H_{92}N_4K_2Si_2Zn_2$: C, 60.85; H, 7.86; N, 5.46. Found: C, 60.78; H, 7.62; N, 5.41.

Synthesis of [K-C222]$_2$[Zn(η^2-SiMe$_2$(NDipp)$_2$)]$_2$, ([K-C222]$_2$[7]). A mixture of **5**

(0.50 g, 0.53 mmol) and Cryptand [2.2.2] (0.40 g, 1.06 mmol) was prepared in 6 mL

of THF in a 20 mL of vial, and the resulting solution was kept at −35 °C. To the

solution was slowly added solid KC_8 (0.21 g, 1.55 mmol) at −35 °C, and the solution

was allowed to warm to room temperature. Vigorous stirring was continuing for 10 h.

The solution was filtered through Celite, and solvent was removed in vacuo from the

filtrate, yielding a white solid. Recrystallization from THF at −35 °C furnished

[K-C222]$_2$[**7**] as colorless crystals (0.74 g, 0.42 mmol, 79% yield in two crops). ^{1}H

NMR (400 MHz, THF-d_8): δ 6.58 (d, 8H, Dipp meta), 6.19 (t, 4H, Dipp para), 4.18

(septet, 8H, C*H*Me$_2$), 3.52 (s, 24H, cryptand), 3.49 (m, 24H, cryptand), 2.50 (m, 24H,

cryptand), 0.92 (d, 48H, CH*Me$_2$*), –0.24 (s, 12H, Si*Me$_2$*). ^{13}C NMR (100.62MHz,

THF-d_8): δ 154.97 (C, Dipp *ipso*), 144.00 (C, Dipp *ortho*), 121.38 (CH, Dipp *meta*),

114.20 (CH, Dipp *para*), 71.30 (C, cryptand), 68.43 (C, cryptand), 54.75 (C,

cryptand), 27.23 (C, Dipp, *C*HMe$_2$), 25.92 (C, CH*Me$_2$*), 6.37 (C, Si*Me$_2$*). Anal. Calcd

for $C_{88}H_{152}N_4K_2O_{12}Si_2Zn_2$: C, 59.40; H, 8.61; N, 6.30. Found: C, 59.17; H, 8.65; N,

6.24.

Crystallographic Structure Determinations. The X-ray crystallographic data

collections for **5**, **6,** and **[K-C222]$_2$[7]** were carried out on a Bruker-Nonius Kappa

CCD four-circle diffractometer with graphite-monochromated Mo Kα radiation (λ =

0.71073 Å) outfitted with a low-temperature, nitrogen-stream aperture. The structures

were solved using direct methods, in conjunction with standard difference Fourier techniques and refined by full-matrix least-squares procedures. A summary of the crystallographic data for complexes **5**, **6,** and **[K-C222]$_2$[7]** is shown in Table *S1*. An empirical absorption correction (multi-scan) was applied to the diffraction data for all structures. All non-hydrogen atoms were refined anisotropically. Unless otherwise specified, all hydrogen atoms were calculated by using the riding model. All software used for diffraction data processing and crystal-structure solution and refinement are contained in the SIR92 or SHELXL 97[1] program suites, respectively.

Crystal structures of complexes **5** and **6** display A alerts accord to CheckCif reports; these alerts are arisen from unsolved disordered problems and squeezing co-crystallized solvent molecules.

Computational Details. Our previous study on the quadruply-bonded complex Mo$_2$(μ-η^2-Me$_2$Si(NDipp)$_2$)$_2$[2] showed that it was impossible to probe the Mo–Mo bond by virtue of DFT calculations using a simplified model, and therefore computations on the basis of the authentic molecular structure **7**$^{2-}$ is engaged. Two-layered ONIOM[3-9] computations, including the second order Mφller-Plesset perturbation theory[10-14] with full-electron correlation (full-MP2) applied to the high layer, as well as density functional theory (DFT) to the low layer, are carried out. The use of DFT method of BP86 by the combination of Becke 88[15] and Pedew 86[16] is due to its superior performance in a literature about the Zn–Zn bonding.[17] The high layer is defined as the central framework of the molecule, Zn$_2$N$_4$Si$_2$, while the entire molecule is assigned into the low layer. The basis set used in the low layer is split-valence 6-31G(d,p), generating 1350 basis functions. This 6-31G(d,p) basis set and its form with double diffuse functions, 6-31G++(d,p), are used with full-MP2 theory in the

high layer producing 210 and 268 basis functions, respectively. The ONIOM theories

are therefore denoted as ONIOM(full-MP2/6-31G(d,p):BP86/6-31G(d,p)) and

ONIOM(full-MP2/6-31G++(d,p):BP86/6-31G(d,p)), and are abbreviated as ONIOM1

and ONIOM2 for short throughout the paper. All of the computations are performed

by virtue of an accelerated version of Gaussian 03 program[18] compiled by Intel

Fortran Compiler.[19,20]

Geometrical optimizations by ONIOM theories are carried out for **5** and **7**$^{2-}$ using

identical definitions in high and low layers, followed by zero-point energy (ZPE)

corrections to confirm their energetical minima. The symmetry of the aforementioned

structures is constrained to C_2 over the course of geometrical minimization. Transition

structures (TS) are located using the synchronous transit-guide quasi-Newton (STNQ)

method[21,22] for the monoanionic in the doublet state as well as the dianionic in the

singlet state. Symmetry constraint is released in search for TS (C_1), and zero-point

energy (ZPE) calculations are followed to confirm the imaginary frequency. Energetic

numeric together with the Zn–Zn bond length of each optimized geometry based on

ONIOM1 and ONIOM2 theories are respectively demonstrated in Tables *S2* and *S3*.

References

1. Sheldrick, G. M. *SHELXTL, Program for Crystal Structure Determination*; Siemens Analytical X-ray Instruments Inc.: Madison, WI, 1994.
2. Tsai, Y.-C.; Lin, Y.-M.; Yu, J.-S. K.; Hwang, J.-K. *J. Am. Chem. Soc.* **2006**, *128*, 13980-13981.
3. Maseras, F.; Morokuma, K. *J. Comput. Chem.* **1995**, *16*, 1170-1179.
4. Humbel, S.; Sieber, S.; Morokuma, K. *J. Chem. Phys.* **1996**, *105*, 1959-1967.
5. Matsubara, T.; Sieber, S.; Morokuma, K. *Int. J. Quant. Chem.* **1996**, *60*, 1101-1109.
6. Svensson, M.; Humbel, S.; Froese, R. D. J.; Matsubara, T.; Sieber, S.; Morokuma, K. *J. Phys. Chem.* **1996**, *100*, 19357-19363.
7. Svensson, M.; Humbel, S.; Morokuma, K. *J. Chem. Phys.* **1996**, *105*, 3654-3661.

8. Dapprich, S.; Komaromi, I.; Byun, K. S.; Morokuma, K.; Frisch, M. J. *J. Mol. Str. Theochem* **1999**, *462*, 1-21.

9. Vreven, T.; Morokuma, K. *J. Comput. Chem.* **2000**, *21*, 1419–1432.

10. Head-Gordon, M.; Pople, J. A.; Frisch, M. J. *Chem. Phys. Lett.* **1988**, *153*, 503-506.

11. Frisch, M. J.; Headgordon, M.; Pople, J. A. *Chem. Phys. Lett.* **1990**, *166*, 275-280.

12. Frisch, M. J.; Headgordon, M.; Pople, J. A. *Chem. Phys. Lett.* **1990**, *166*, 281-289.

13. Headgordon, M.; Headgordon, T. *Chem. Phys. Lett.* **1994**, *220*, 122-128.

14. Saebo, S.; Almlof, J. *Chem. Phys. Lett.* **1989**, *154*, 83-89.

15. Becke, A. D. *Phys. Rev. A* **1988**, *38*, 3098-3100.

16. Perdew, J. P. *Phys. Rev. B* **1986**, *33*, 8822-8824.

17. Wang, Y. Z.; Quillian, B.; Wei, P. R.; Wang, H. Y.; Yang, X. J.; Xie, Y. M.; King, R. B.; Schleyer, P. V.; Schaefer, H. F.; Robinson, G. H. *J. Am. Chem. Soc.* **2005**, *127*, 11944-11945.

18. Gaussian 03, Rev. D.01, Frisch, M. J.; Trucks, G. W.; Schlegel, H. B.; Scuseria, G. E.; Robb, M. A.; Cheeseman, J. R.; Montgomery, Jr., J. A.; Vreven, T.; Kudin, K. N.; Burant, J. C.; Millam, J. M.; Iyengar, S. S.; Tomasi, J.; Barone, V.; Mennucci, B.; Cossi, M.; Scalmani, G.; Rega, N.; Petersson, G. A.; Nakatsuji, H.; Hada, M.; Ehara, M.; Toyota, K.; Fukuda, R.; Hasegawa, J.; Ishida, M.; Nakajima, T.; Honda, Y.; Kitao, O.; Nakai, H.; Klene, M.; Li, X.; Knox, J. E.; Hratchian, H. P.; Cross, J. B.; Bakken, V.; Adamo, C.; Jaramillo, J.; Gomperts, R.; Stratmann, R. E.; Yazyev, O.; Austin, A. J.; Cammi, R.; Pomelli, C.; Ochterski, J. W.; Ayala, P. Y.; Morokuma, K.; Voth, G. A.; Salvador, P.; Dannenberg, J. J.; Zakrzewski, V. G.; Dapprich, S.; Daniels, A. D.; Strain, M. C.; Farkas, O.; Malick, D. K.; Rabuck, A. D.; Raghavachari, K.; Foresman, J. B.; Ortiz, J. V.; Cui, Q.; Baboul, A. G.; Clifford, S.; Cioslowski, J.; Stefanov, B. B.; Liu, G.; Liashenko, A.; Piskorz, P.; Komaromi, I.; Martin, R. L.; Fox, D. J.; Keith, T.; Al-Laham, M. A.; Peng, C. Y.; Nanayakkara, A.; Challacombe, M.; Gill, P. M. W.; Johnson, B.; Chen, W.; Wong, M. W.; Gonzalez, C.; and Pople, J. A.; Gaussian, Inc., Wallingford CT, 2004.

19. Yu, J.-S. K.; Hwang, J.-K.; Tang, C.-Y.; Yu, C.-H. *J. Chem. Inf. Comput. Sci.* **2004**, *44*, 635-642.

20. Yu, J.-S. K.; Yu, C.-H. *J. Chem. Inf. Comput. Sci.* **2002**, *42*, 673-681.

21. Peng, C. Y.; Ayala, P. Y.; Schlegel, H. B.; Frisch, M. J. *J. Comput. Chem.* **1996**, *17*, 49-56.

22. Peng, C. Y.; Schlegel, H. B. *Isr. J. Chem.* **1993**, *33*, 449.

Table *S1*. Crystallographic Data for **5, 6,** and [K-C222]$_2$**[7]**

compound	**5**	**6**	[K-C222]$_2$**[7]**
empirical formula	$C_{56}H_{88}N_4OSi_2Zn_2$	$C_{52}H_{80}K_2N_4Si_2Zn_2$	$C_{100}H_{176}K_2N_8O_{15}Si_2Zn_2$
fw	1020.22	1026.32	1995.61
crystal system	Triclinic	Tetragonal	Triclinic
space group	$P{-}1$	$I{-}4$	$P{-}1$
a (Å)	13.1906(2)	23.7530(7)	13.9744(3)
b (Å)	20.2619(4)	23.7530(7)	15.0000(3)
c (Å)	21.1216(4)	20.8380(9)	29.4819(8)
α (deg)	86.1410(10)	90	97.4280(10)
β (deg)	76.3280(10)	90	94.2870(10)
γ (deg)	85.5180(10)	90	98.8750(10)
vol (Å^3)	5461.42(17)	11756.9(7)	6026.2(2)
Z	4	8	2
d (calc. g/cm^3)	1.241	1.160	1.100
μ (mm^{-1})	0.963	1.032	0.542
temperature (K)	200	200	200
final R indices	R1 = 0.0604	R1 = 0.0820	R1 = 0.0963
[I > 2σ(I)]^{a,b}	*w*R2 = 0.1695	*w*R2 = 0.1866	*w*R2 = 0.2257
R indices	R1 = 0.0979	R1 = 0.1458	R1 = 0.2256
(all data)	*w*R2 = 0.1856	*w*R2 = 0.2404	*w*R2 = 0.2711

[a]$R1 = \Sigma||F_o| - |F_c||/\Sigma|F_o|$. [b]$wR2 = [\Sigma[w(F_o^2 - F_c^2)^2]/\Sigma w(F_o^2)^2]^{1/2}$, $w = 1/[\sigma^2(F_o^2) + (aP)^2 + bP]$, where $P = [\max(F_o^2 \text{ or } 0) + 2(F_c^2)]/3$

Table S2. Optimized Zn–Zn bond lengths and energies using ONIOM(full-MP2/6–31G(d,p):BP86/6-31G(d,p)). The high layer is defined as $Zn_2N_4Si_2$ and the low layer is the entire molecule. PMP2 denotes the spin-projected MP2 energy and only applies to doublet state

ONIOM(full-MP2/6-31G(d,p):BP86/6-31G(d,p)

species	5	5$^-$	7$^-$	5^{2-}	IM$^-$	TS^{2-}	7^{2-}
charge, multiplicity	0, 1	-1, 2	-1, 2	-2, 1	-1, 2	-2, 1	-2, 1
Zn–Zn bond length (Å)	2.604	2.362	2.405	2.238	2.963	2.352	2.323
BP86 (a.u.)	–4361.6481668	–4361.6348821	–4361.5928336	–4361.4684909	–4361.6246770	–4361.5266628	–4361.5359623
ZPE (a.u.)	1.1793056	1.1762216	1.1763309	1.1710723	1.1770168	1.1729829	1.1734306
BP86 w/ZPE (a.u.)	–4360.4688612	–4360.4586605	–4360.4165027	–4360.2974186	–4360.4476602	–4360.3536799	–4361.3625317
R/UMP2 (a.u.)	–4357.0400406	–4357.0049321	–4356.9581146	–4356.8190555	–4357.0067917	–4356.8849569	–4356.8966142
PMP2 (a.u., doublet)	---	–4357.0058122	–4356.9589582	---	–4357.0071056	---	---
R/UMP2 w/ZPE (a.u.)	–4355.8607350	–4355.8287105	–4355.7817837	–4355.6479832	–4355.8297749	–4355.7119740	–4355.7231836
PMP2 w/ZPE (a.u., doublet)	---	–4355.8295906	–4355.7826273	---	–4355.8300888	---	---
ΔE_{MP2} (kcal/mol)	0.00	20.096	49.543	133.504	19.428	93.349	86.315
ΔE_{BP86} (kcal/mol)	0.00	6.401	32.855	107.582	13.304	72.277	66.723
imaginery frequency (cm^{-1})	---	–53.2	---	–66.01	–183.543	–134.423	---

Table S3. Optimized Zn–Zn bond lengths and energies using ONIOM (full-MP2/6–31++G(d,p):BP86/6-31G(d,p)). The high layer is defined as $Zn_2N_4Si_2$ and the low layer is the entire molecule. PMP2 denotes the spin-projected MP2 energy and only applies to doublet state. Geometry optimization of $\mathbf{5}^{2-}$ was not successful at this level, and therefore the geometry optimized at ONIOM (full-MP2/6–31++G(d,p):BP86/6-31G(d,p)) was used.

ONIOM(full-MP2/6-31++G(d,p):BP86/6-31G(d,p)

| species	**5**	**5$^-$**	**7$^-$**	**5^{2-}**	**IM$^-$**	**7^{2-}**	
charge, multiplicity	0, 1	-1, 2	-1, 2	-2, 1	-1, 2	-2, 1	
Zn–Zn bond length (Å)	2.712	2.458	2.504	ONIOM1	3.064	2.374	
BP86 (a.u.)	–4361.6465014	–4361.6312883	–4361.5881224	–4361.4684909	–4361.6204307	–4361.5311897	
ZPE (a.u.)	1.1778776	1.1747011	1.1758499	1.1710723	1.1763627	1.172646	
BP86 w/ZPE (a.u.)	–4360.4686238	–4360.4565822	–4360.4122725	–4360.2974186	–4360.4440680	–4361.3585437	
R/UMP2 (a.u.)	–4357.3281617	–4357.3174106	–4357.2782909	–4357.1979084	–4357.3181102	–4357.2458559	
PMP2 (a.u., doublet)	---	–4357.3183852	–4357.2792160	---	–4357.3185833	---	---
R/UMP2 w/ZPE (a.u.)	–4356.1502841	–4356.1427095	–4356.1024410	–4356.0268361	–4356.1417475	–4356.0732099	
PMP2 w/ZPE (a.u., doublet)	---	–4356.1436841	–4356.1033661	---	–4356.1422206	---	
ΔE_{MP2} (kcal/mol)	0.00	4.753	30.022	77.465	5.357	51.648	
ΔE_{BP86} (kcal/mol)	0.00	7.556	35.361	107.433	15.409	69.076	
imaginery frequency (cm^{-1})	---	---	---	---	---	---	
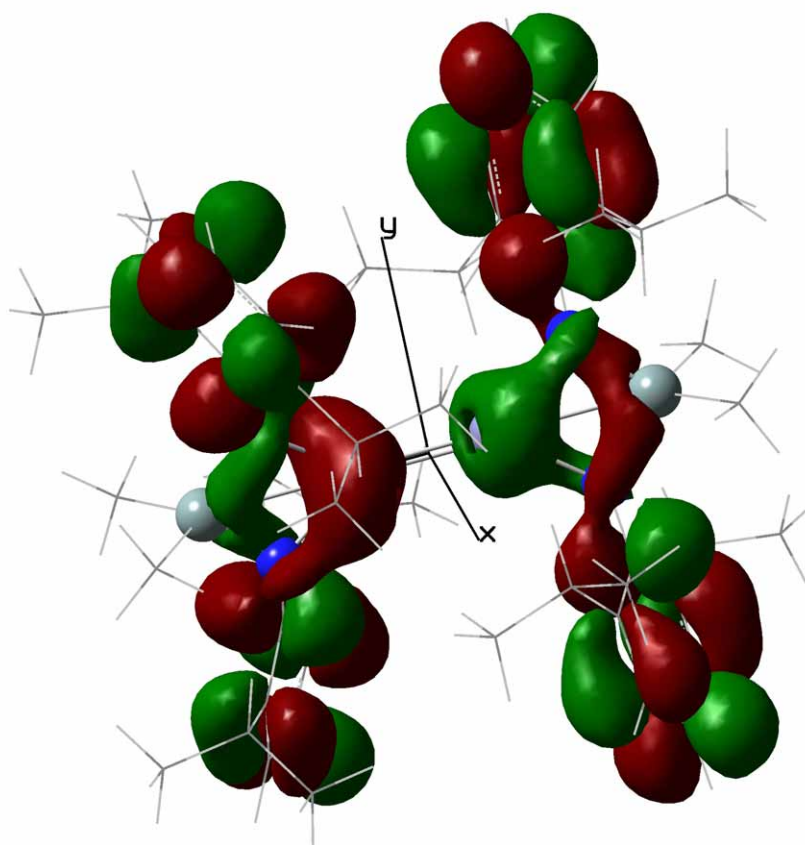
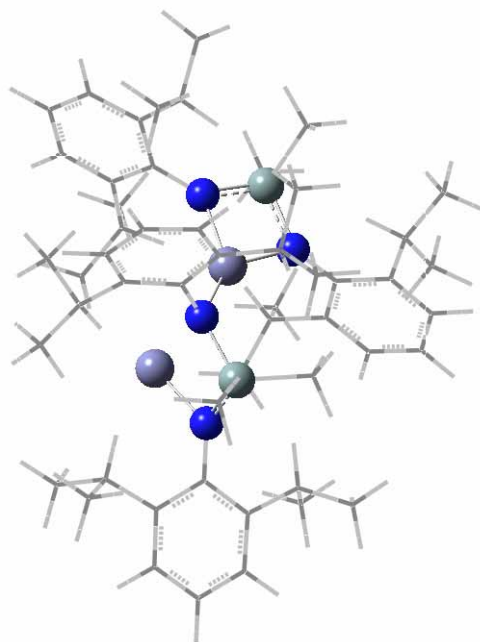*Figure S1*. The contour plot of LUMO+5 of 7^{2-}.

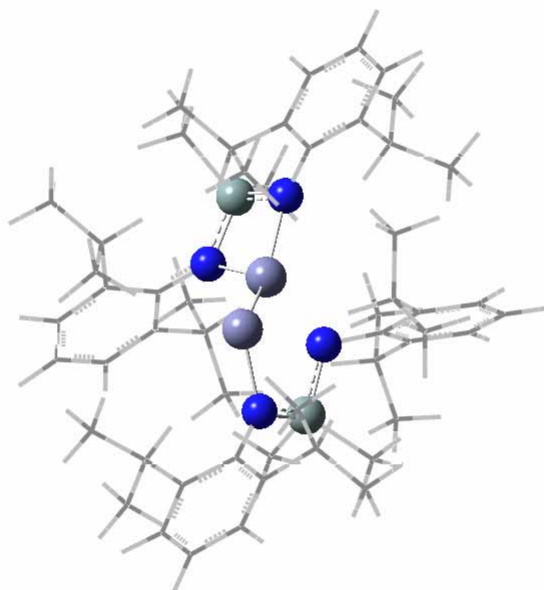*Figure S2*. The computed structure of the intermediate **IM⁻** in which the Zn-Zn distance is computed to be 3.064 Å.

Figure S3. The computed structure of the transition state **TS**$^{2-}$.